Future of land surface water availability over the Mediterranean basin and North Africa: Analysis and synthesis from the CMIP6 exercise

Khadija Arjdal, Fatima Driouech, Étienne Vignon, Frédérique Chéruy, Rodrigo Manzanas, Philippe Drobinski, Abdelghani Chehbouni, Abderrahmane Idelkadi

Received: 21 December 2022 | Revised: 6 May 2023 | Accepted: 12 June 2023

DOI: 10.1002/asl.1180

RESEARCH ARTICLE

Atmospheric Science Letters RMetS

Future of land surface water availability over the Mediterranean basin and North Africa: Analysis and synthesis from the CMIP6 exercise

Khadija Arjdal[1,2] | **Fatima Driouech**[1] | **Étienne Vignon**[2] | **Frédérique Chéruy**[2] | **Rodrigo Manzanas**[3,4] | **Philippe Drobinski**[2] | **Abdelghani Chehbouni**[1] | **Abderrahmane Idelkadi**[2]

[1]International Water Research Institute (IWRI), CSAES - Mohammed VI Polytechnic University, Benguerir, Morocco

[2]Laboratoire de Météorologie Dynamique-IPSL, Sorbonne Université/CNRS/École Normale Supérieure-PSL Université/École Polytechnique-Institut Polytechnique de Paris, Paris, France

[3]Departamento de Matemática Aplicada y Ciencias de la Computación (MACC), Universidad de Cantabria, Santander, Spain

[4]Grupo de Meteorología y Computación, Universidad de Cantabria, Unidad Asociada al CSIC, Santander, Spain

Correspondence
Khadija Arjdal, International Water Research Institute (IWRI), Mohammed VI Polytechnic University, Benguerir, Morocco.
Email: khadija.arjdal@um6p.ma

Funding information
Université Mohammed VI Polytechnique

Abstract

The Mediterranean basin and Northern Africa are projected to be among the most vulnerable areas to climate change. This research documents, analyzes, and synthesizes the projected changes in precipitation P, evapotranspiration E, net water supply from the atmosphere to the surface P–E, and surface soil moisture over these regions as simulated by 17 global climate models from the sixth exercise of the Coupled Model Intercomparison Project (CMIP6) under two Shared Socioeconomic Pathways, SSP2-4.5, and SSP5-8.5. It also explores the sensitivity of the results to the chosen climate scenario and model resolution and assesses how the projections have evolved from the fifth exercise (CMIP5). Models project a statistically robust drying over the entire Mediterranean and coastal North Africa. Over the Northern Mediterranean sector, a significant precipitation decrease reaching -0.4 ∓ 0.1 mm day^{-1} is projected during the 21st century under the SSP5-8.5 scenario. Conversely, a significant increase in precipitation of $+0.05$ to 0.3 ∓ 0.1 mm day^{-1} is projected over South-Eastern Sahara under the same scenario. Evapotranspiration and soil moisture exhibit decreasing trends over the Mediterranean basin and an increase over the Sahara for both SSPs, with a notable acceleration from the 2020s. As a result, P-E is projected to decrease at a rate of about -0.3 mm day^{-1} under the high-end scenario SSP5-8.5 over the Mediterranean whilst no significant changes are expected over the Sahara due to evapotranspiration compensation effects. CMIP6 and CMIP5 models project qualitatively similar patterns of changes but CMIP6 models exhibit more intense changes over the Mediterranean basin and South-Eastern Sahara, especially during winter.

KEYWORDS

CMIP5, CMIP6, evapotranspiration, Mediterranean, North Africa, precipitation

1 | INTRODUCTION

Climate projections indicate that the Mediterranean and adjacent Northern Africa are among the most vulnerable areas to global warming (Almazroui et al., 2020; Lee et al., 2020), specifically regarding the hydrological cycle (Hanel et al., 2018) and heat extremes (Seneviratne et al. 2021). The intensity of climate change in the Mediterranean region and the associated high socio-economical risks raised the necessity of establishing the First Mediterranean Assessment Report (Cherif et al., 2020). Moreover, the recent sixth Assessment Report of the Intergovernmental Panel on Climate Change (IPCC) stresses that "there is high confidence that anthropogenic forcings are causing increased aridity and drought severity in the Mediterranean region" (Douville & John, 2021). Subsequently, potential stress on water resources are projected over the Southern Mediterranean region (Prudhomme et al., 2014), consistently with a projected decrease in surface water resources in North Africa under various climatic scenarios owing to precipitation reduction and evapotranspiration increase (Balhane et al., 2021; Driouech et al., 2010; Tramblay et al., 2018). Therefore, assessing the water cycle and surface hydrology response to global warming in water-stressed areas such as North Africa and the Southern Mediterranean region is crucial for anticipating consequences on water supplies, agriculture, and ecosystems (Marchane et al., 2017; Tramblay et al., 2018).

Global climate models (GCMs), and in particular those included in the Coupled Model Intercomparison Projects (CMIP; IPCC 2021), are commonly-used tools to assess the future effects of climate change on the water cycle and particularly on the different terms of the surface water budgets. In a CMIP5 (fifth CMIP phase)-based study, Mariotti et al., (2015) found a significant decrease in mean precipitation over southern areas of the Mediterranean during winter under a moderate greenhouse gas emission scenario. Lionello & Scarascia (2018) report a decrease of 4% per degree of warming in annual precipitation over the Mediterranean area according to CMIP5 models under the high-emission RCP8.5 scenario. Mariotti et al. (2015) found a precipitation reduction during summer over Spain, western Northern Africa, and Turkey along with a projected increase in winter evapotranspiration over Northern Mediterranean land by the end of the 21st-century relative to the 1980–2005 reference period.

Precipitation (P) minus evapotranspiration (E) (P–E hereafter) represents the net freshwater flux from the atmosphere to the surface as defined by Byrne and O'Gorman (2015), and is also called "water availability." P–E drives the water percolation and soil moisture (SM), the run-off, and ultimately the river flow and groundwater recharge. The climatological P–E is close to zero over Mediterranean (MED hereafter) lands except in Northern areas during winter where P surpasses E (Mariotti et al., 2015). CMIP5 projections indicate a general decreasing trend for P–E across MED lands, specifically during summer due to the precipitation decrease over Northern areas (Mariotti et al. 2015). Assessing future changes in surface SM is also critical to anticipate the impact of changes of the hydrological cycle on several socio-economical activities such as agriculture (Ruosteenoja et al., 2018; Seneviratne et al., 2010), especially in arid and semi-arid areas. Over the Mediterranean basin, CMIP5 models simulate a continuous reduction in total soil moisture during the twentieth century, and it is expected to persist throughout the 21st-century (Mariotti et al., 2015).

In addition to GCMs, regional climate models (RCMs) laterally forced with GCMs are also employed to provide scenarios at higher resolutions over a specific area. Climate change impacts across the MED area have been estimated from RCM simulations in the framework of the Coordinated Regional Climate Downscaling Experiment database (Drobinski et al., 2020; McSweeney et al., 2015; Tebaldi et al., 2005). Tuel et al. (2021) underlined the necessity of carefully selecting the GCMs used to force the RCM to properly project the climate over the MED region. Hence the need to select carefully and analyze the surface water projections and related uncertainties across the Mediterranean and North Africa from recent GCM simulations.

In this paper, we provide an in-depth analysis and synthesis of the surface water supply projections from the newly available CMIP6 GCMs—which show considerable improvements in terms of spatial resolution and physics with respect to CMIP5 (Eyring et al. 2016)—over MED and Saharan (SAH hereafter) subregions. For this purpose, we analyze the quantitative evolution of precipitation, evapotranspiration, P–E, and surface SM over those two regions for a carefully-selected set of simulations and thoroughly discuss the ensemble statistics. Note that evaluating RCM scenarios over MED and SAH is beyond the scope of the present paper, but our study will help better assess the suitability of future projections from the last generation global projections as boundary conditions for RCM runs.

2 | DATA AND METHODS

We considered 17 GCMs involved in the CMIP6 database (https://esgf-node.llnl.gov/search/cmip6/) and analyzed the "historical" (1850–2014) simulations (Eyring et al., 2016) and the low and high-end forcing Shared Socio-economic Pathways "SSP2-4.5" and "SSP5-8.5"

TABLE 1 List and characteristics of CMIP6 models used in this study.

Model	Original horizontal resolution (lon × lat)	Run	References
BCC-CSM2-MR	1.1° × 1.1°	r1i1p1f1	Wu et al. (2019)
CAMS-CSM1-0	1.1° × 1.1°	r2i1p1f1	Rong et al. (2019)
CESM2	1.3° × 0.9°	r4i1p1f1	Lauritzen et al. (2018)
CESM2-WACCM	1.3° × 0.9°	r1i1p1f1	Li (2019)
CMCC-CM2-SR5	0.9° × 1.2°	r1i1p1f1	Cherchi et al. (2018)
MPI-ESM1-2-HR	0.9° × 0.9°	r1i1p1f1	Gutjahr et al. (2019)
MRI-ESM2-0	1.1° × 1.1°	r1i1p1f1	Yukimoto et al. (2019)
NorESM2-MM	1.2° × 0.9°	r1i1p1f1	Seland et al. (2020)
TaiESM1	0.9° × 1.25°	r1i1p1f1	Lee et al. (2020)
CNRM-CM6-1	1.4° × 1.4°	r1i1p1f2	Voldoire et al. (2019)
CNRM-ESM2-1	1.4° × 1.4°	r1i1p1f2	Séférian et al. (2019)
GISS-E2-1-G	2° × 2.5°	r1i1p1f2	Kelley et al. (2020)
IPSL-CM6A-LR	2.5° × 1.3°	r1i1p1f1	Boucher et al. (2020)
MIROC6	1.4° × 1.4°	r1i1p1f1	Tatebe et al. (2019)
MPI-ESM1-2-LR	1.9° × 1.9°	r1i1p1f1	Mauritsen et al. (2019)
NorESM2-LM	2.5° × 1.9°	r1i1p1f1	Seland et al. (2020)
UKESM1-0-LL	1.9° × 1.3°	r1i1p1f2	Sellar et al. (2019)

Note: Models with a native resolution close to 100-km (250 km) are shown in blue (red).

(2015–2100) simulations from ScenarioMIP (O'Neill et al., 2016). The models' selection was based on the availability of the following output variables at the time of the study: 2-m temperature, precipitation rate, evapotranspiration, and surface SM content (top 10 cm) over the period 1850–2100 (historical + scenarios) (Table 1). Three models considering enclosed marginal seas as "land" have further been excluded to avoid inconsistencies in the multi-model land evapotranspiration statistics. Following Agosta et al. (2015) we have briefly assessed the performance of the selected model to simulate the large-scale climate patterns driving the MED and SAH climate (see Figure S8 in Section B of the supplement). None of the models considered here outperforms or lies outside the others but models with a higher horizontal resolution generally show better performance in terms of large-scale circulation metrics. For a thorough evaluation of CMIP6 models over the Mediterranean and African regions in terms of near-surface climate, we also refer the readers to Babaousmail et al. (2021); Bağçaci et al. (2021); Seker & Gumus (2022). For the sake of fairness in our comparative study, we selected the available set of climate models from CMIP5 and its updated version of CMIP6 (Table S1). We will also briefly comment on the behavior of the total SM content. SM contents will be expressed as relative rather than absolute quantities since the soil schemes of the different models and especially their depths vary (Cook et al., 2020). Analyses are conducted over the MED and Sahara (SAH) subregions as defined for the IPCC's sixth assessment (Iturbide et al., 2020), as shown in Figure 1a.

Northern and Southern shores of the Mediterranean Sea are expected to exhibit quite different quantitative responses to climate change (Tuel et al., 2021), We, therefore, subdivide the MED sector into two sub-regions for our analyses: the Northern (N_MED, northern than 35°N) and Southern (S_MED) Mediterranean (see Figure 1a).

In order to assess uncertainties and identify robust signals in future model projections, we calculated the multimodel ensemble mean and variance across models. As the large-scale circulation fields over the MED and SAH regions seem to be resolution dependent (Section B of the supplement), we will separately consider two groups of models depending on their resolution (Table 1): one group for which the native horizontal resolution is close to ∼100 km and another one for which it is close to ∼250 km. Given that our work focuses on land, we masked out grid boxes where the land area fraction is less than 90%. This later has been chosen as a trade-off to conserve the largest possible study area avoiding retaining meshes at the continent margins for which the evapotranspiration flux is not representative for land surfaces (Figures S1 and S2). For assessing the statistical robustness of future changes (or non-changes), we use the non-parametric Wilcoxon–Mann–Whitney test comparing future (2071–2100) and historical (1981–2010) data for

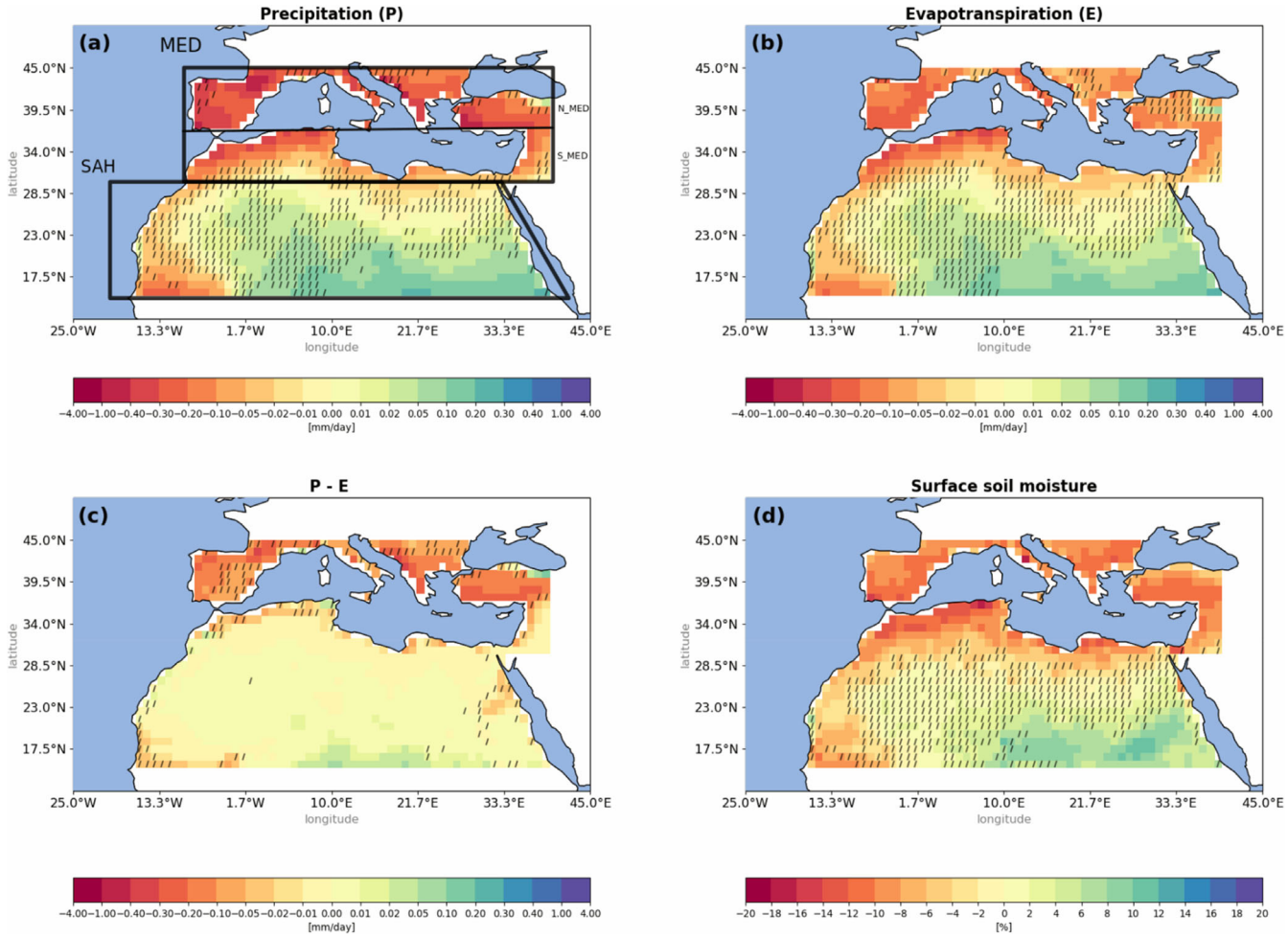

FIGURE 1 Future changes in the 100-km ensemble-mean annual precipitation (mm day^{-1}), evapotranspiration (mm day^{-1}), P–E (mm day^{-1}), and surface soil moisture (%) over the Mediterranean basin and the Sahara under the SSP5-8.5 scenario for 2071–2100 with respect to 1981–2010. The slashes correspond to grid boxes exhibiting nonrobust changes based on the nonparametric Wilcoxon–Mann–Whitney test with a 95% threshold.

each individual model. An increase or a decrease is deemed statistically robust if at least two-thirds of the models project significant (i.e., the *p*-value of the Wilcoxon–Mann–Whitney test <= 0.05) changes that agree on the sign. Unlike the robustness tests used in IPCC (2021), we also consider a constant response to be robust if at least two-thirds of the models exhibit a non-statistically significant change.

3 | RESULTS AND DISCUSSION

3.1 | Spatial patterns of future changes of precipitation, evapotranspiration, P-E, and surface moisture for the SSP2-4.5 and SSP5-8.5 scenarios

Figures 1, 2 show the 100-km ensemble-mean annual changes under SSP5-8.5 and SSP2-4.5 scenarios respectively. The projected changes—calculated as the difference between the 2071–2100 and 1981–2010 periods—show reduced precipitation over MED and all along the Atlantic coasts of Morocco and Mauritania. Figures 1a, 2a show a robust decrease of precipitation reaching −0.4 (−0.3) mm day^{-1} across the western part of MED and nearly −0.1 to −0.02 (respectively, −0.05 to −0.01) mm day^{-1} in the eastern part, mostly in Libya and Egypt for the SSP5-8.5 (respectively, SSP2-4.5) scenario ensembles. The increase in precipitation over the South-Eastern SAH ranges between +0.05 to 0.3 (respectively, +0.01 to 0.3) mm day^{-1} by the end of the century for high (medium)-end scenario emission. This concurs with Waha et al., (2017) who showed that a projected northward shift of the inter-tropical convergence zone (ITCZ) will enhance moisture transfer to the Southern Middle East and North Africa. CMIP6 models also project a robust northward shift of the ITCZ over eastern Africa, mostly between May and October (Mamalakis et al., 2021). Our results show that precipitation changes are more pronounced under the

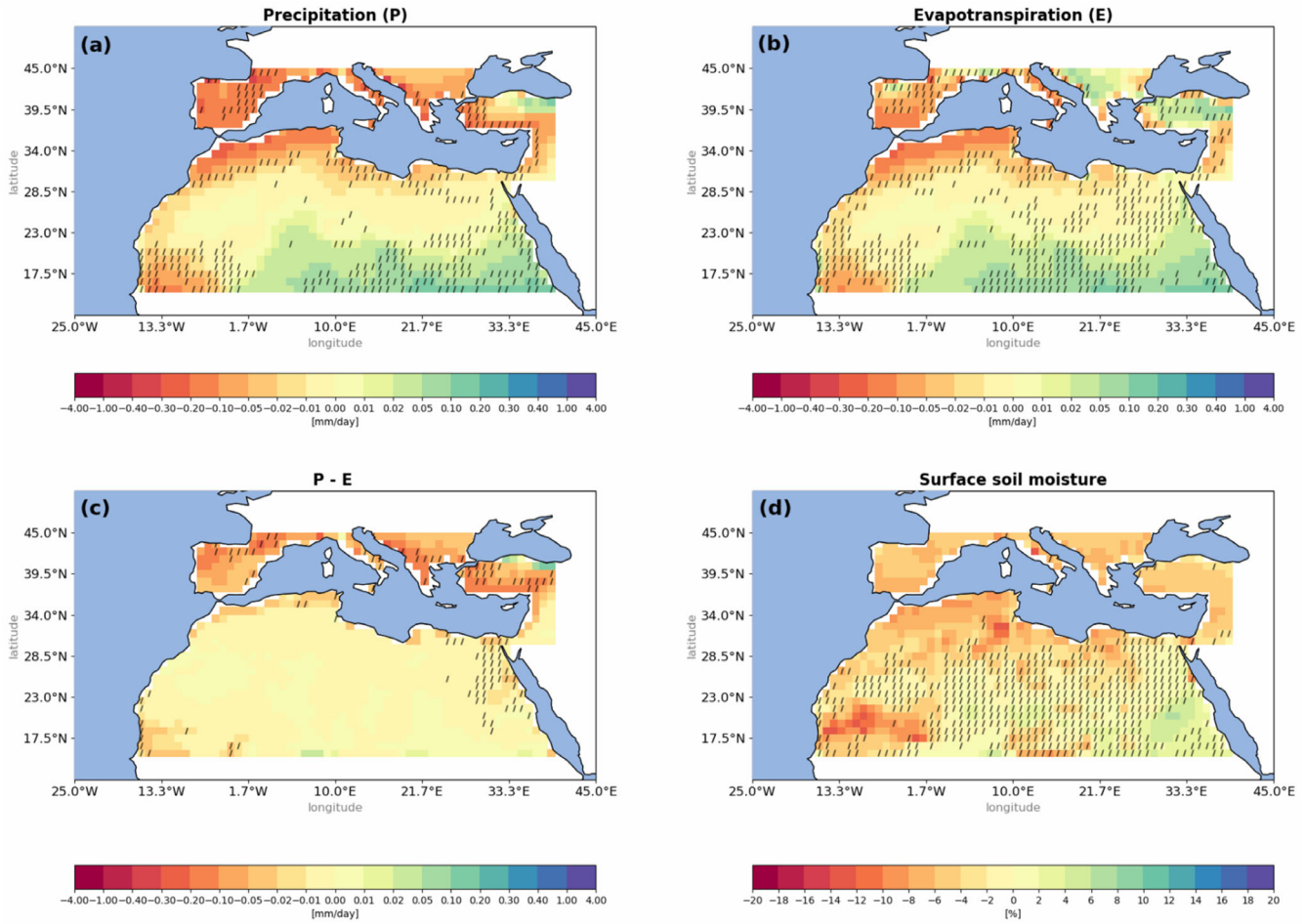

FIGURE 2 Same as Figure 1 but for the SSP2-4.5 scenario.

SSP5-8.5 scenario. Consistently, a statistically robust decrease in evapotranspiration is also projected over the whole Mediterranean region (Figures 1b, 2b), especially over the Iberian Peninsula (IP) and Northern Africa. The projected changes range from −0.05 to −0.3 (respectively, −0.01 to −0.2) mm day^{-1} over Spain, Northern Morocco, Algeria, and Tunisia, with less intense changes not exceeding ∼ −0.05 (respectively, −0.02) mm day^{-1} projected over Egypt, Syria, and Turkey for the SSP5-8.5 (respectively, SSP2-4.5) scenario, in addition to positive changes (∼ + 0.02 mm day^{-1}) over Greece and Southern Black sea borders under the medium-end scenario. As shown in Mariotti et al. (2015), this decrease in evapotranspiration over the MED region can be mostly explained by the decrease in precipitation that reduces the SM content available for evapotranspiration. An increase in evapotranspiration (+0.02 to +0.20 mm day^{-1}), corresponding to a relative change of about +10% to 50%, is projected over SAH, in Southern Egypt, Libya, and Sudan, for both scenarios.

Regarding P–E (Figures 1c, 2c), there is an overall projected decrease over MED, more pronounced in the European part. The projected changes range between −0.05 and −0.3 (respectively, −0.02 and −0.2) mm day^{-1} over the IP, Italy, and Turkey under the SSP5-8.5 (respectively, SSP2-4.5) scenario, which corresponds to a relative evolution of approximately −20%. However, Northern Africa already characterized by a climatological P–E close to zero, exhibits weaker change signals (∼ ±0.01) with a slight positive P–E in far south SAH.

Consistently with P and E responses, an overall decrease in SM (Figures 1d, 2d) is simulated. The projected changes in SM reach −12 (−8)% in parts of Spain, Northern Morocco, and Algeria for the SSP5-8.5 (SSP2-4.5) scenario. However, large parts of SAH show nonrobust changes especially under the SSP2-4.5 scenario, while about +10% changes can be pointed out in the far south of SAH under the SSP5-8.5 scenario. The total SM shows similar evolution (Figure S3), with changes from −6 to −12 (respectively, −4 and −8) % over MED, and from +6 to +20 (respectively, +4 to +14) % over Southern SAH under the SSP5-8.5 (respectively, SSP2-4.5) scenario, with the strongest change much more localized in the IP, Italy, Northern Morocco, and Algeria. While P–E is close to zero, the relative SM changes in North Africa are significant.

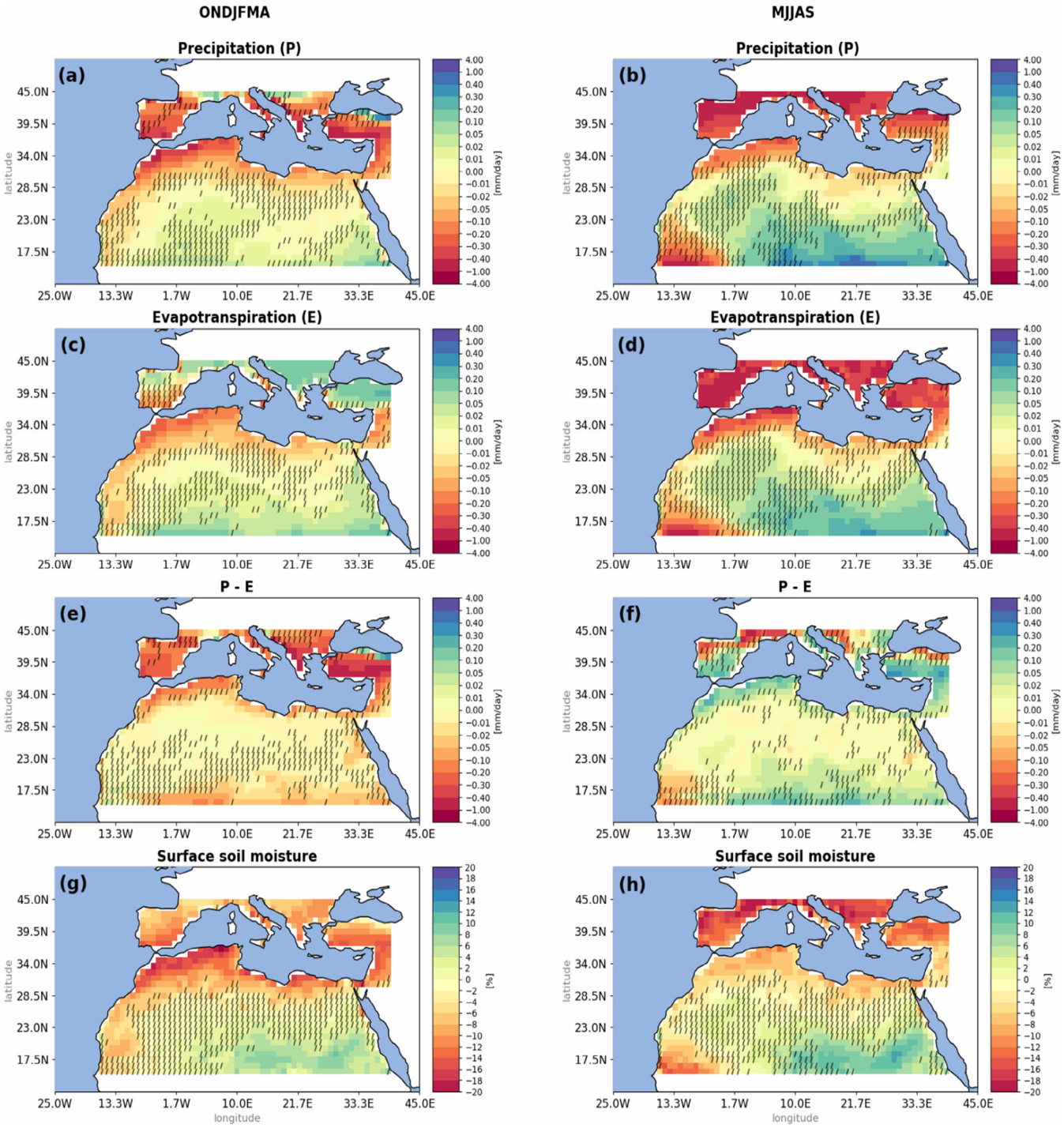

FIGURE 3 As Figure 1 but for the extended boreal winter (left panel) and summer (right panel) seasons under the SSP5-8.5 scenario.

Our results thus show a robust decrease in future water availability over MED due to the decreasing precipitation over the region. However, despite the robust wetting signal for precipitation in South-Eastern Sahara, a near-zero change in the freshwater flux is projected owing to the response of evapotranspiration. Model ensembles exhibit a general south-to-north soil drying, and the inspection of the individual models behavior reveals that most models reproduce this general pattern (Figure S4), with the exception of the GISS-E2-1-G model that projects extensive drying over the entire study area.

3.2 | Seasonal aspects

Since the rainy season in the Mediterranean starts from October and extends to approximately April

(Driouech, 2010; Xoplaki, 2002), separate analyses are conducted for extended boreal winter (ONDJFMA) and summer (MJJAS) for the SSP5.8–5 scenario. The projected 21st-century precipitation decrease is especially intense for the N_MED in MJJAS and for S_MED in ONDJFMA. Increases in precipitation over SAH are twice more intense in summer than in winter (Figure 3a, b). In the Iberian Peninsula, Turkey, and northwestern Maghreb, the precipitation reduction under SSP5-8.5 scenario (Figure 3a, b) reaches -0.2 mm day^{-1} to -0.4 mm day^{-1} during wintertime. While summertime results point to -0.2 mm day^{-1} over Northern Maghreb, and exceed -4 mm day^{-1} in N_MED. This significant decrease in wet-season precipitation throughout the S_MED sector is consistent with previous studies (Diffenbaugh & Giorgi, 2012; Tuel & Eltahir, 2020). The increase in annual precipitation over SAH found in Section 3.1 is most pronounced during summer which concurs with the study of Almazroui et al. (2020). Summertime changes over SAH vary between $+0.3$ and $+4$ mm day^{-1}. Summertime evapotranspiration signal (Figure 3c, d) follows the precipitation behavior with a projected decrease reaching -0.4 mm day^{-1} over MED and an increase of about $+0.4$ mm day^{-1} over South-Eastern Sahara. However, wintertime changes for S_MED are about $+0.2$ mm day^{-1}, -0.2 mm day^{-1} in Northern Maghreb, and around $+0.1$ mm day^{-1} in Southern SAH. P–E (Figure 3e, f) shows an opposite sign between summer and winter over almost the study area, with decreasing changes over the Mediterranean (~ -0.3 mm day^{-1}) and Southern Sahara (~ -0.1 mm day^{-1}) during winter, and increasing changes during summer ($\sim +0.2$ mm day^{-1}) over MED and Southern SAH. Surface SM (Figure 3g, h) follows the same behavior to a large extent. The projected changes reach -16 (-8)% during the extended winter (respectively, summer) over Northern Africa, and -8 (-18)% over the IP, Italy, Greece, and Turkey. Changes across SAH vary from $+10$% during winter to $+14$% during summer.

Results from SSP2-4.5 are shown in Figure S5 in the supplement. Seasonal changes exhibit similar behavior mainly during summer, with reduced intensity, compared to the SSP5-8.5 during winter.

3.3 | Regional assessment and impact of spatial resolution

3.3.1 | Time evolution by region

We now examine more in detail the time evolution of P, E, P–E, and SM, spatially averaged over the N_MED, S_MED, and SAH sectors for the extreme SSP5-8.5 scenario. Figure 4 shows the evolution of the mean annual anomalies and evidences the acceleration of the Mediterranean drying and saharan moistening from the 2020s. The amplitude of change is generally greater in N_MED than in S_MED, mainly due to the higher mean annual precipitation in the Mediterranean, which conditions the evaporation and P–E changes. Figure 4 also shows a gradual decrease in SM during the study period over the entire MED where projected anomalies are around -15% over both N_MED and S_MED, while the evolution over SAH shows a near-zero trend until the 2000s when a slight increase of $+2.5$% emerges.

Results corresponding to the SSP2-4.5 scenario (Figure S6) show similar behavior with less intermodel spread, particularly for the surface SM.

3.3.2 | Spatial resolution impact

Given the sharp topographic and land surface-type contrasts of the MED regions, regional-scale climate change projections in this region are expected to depend on the model resolution (Ashfaq et al., 2016). We conduct a preliminary analysis by separating a $\sim$ 100-km resolution CMIP6 simulation ensemble from that with a $\sim$ 250-km resolution.

While the 250-km resolution and the 100-km resolution ensembles agree over the "historical" period (Figure 4), their future projections show statistically significant differences in precipitation, exceeding 0.1 mm day^{-1} over MED. The lower resolution generally yields more pronounced changes and intermodel variability over MED, while this behavior is less marked over SAH. For almost all the studied variables, the intermodel variability increases with time and decreases with resolution for both shores of the Mediterranean Sea. The differences between the high and low-resolution ensembles also increased toward the end of the century. Unlike MED, the lowest resolution exhibits less intermodel variability over SAH. SM signal shows that less intermodel spread characterizes the highest resolution for almost the entire area. A quite similar behavior is also shown in total SM (Figure S7), except for N_MED, where the 100-km ensemble intermodel variability exceeds that of 250 km. This can be explained by the higher magnitude of total SM which reaches $\sim$2000 kg m^{-2}, while it varies from 500 to 800 kg m^{-2} in the rest of the study area.

3.4 | Temperature- versus scenario-dependent Mediterranean drying and Saharan moistening

Our results and previous studies project a strong drying trend over the Mediterranean region and a substantial

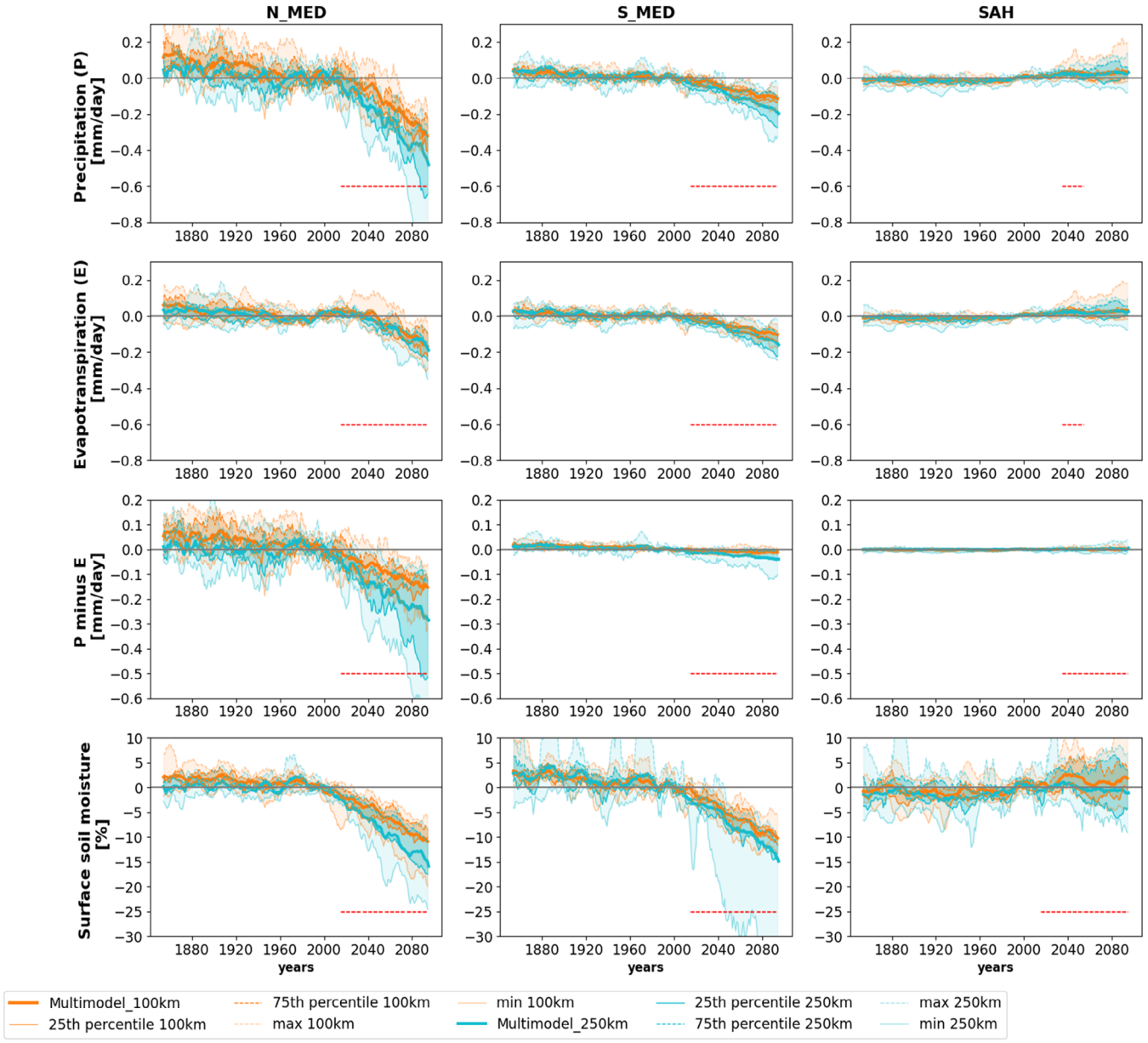

FIGURE 4 Spatially-averaged mean annual changes in precipitation (mm day^{-1}), evapotranspiration (mm day^{-1}), P–E (mm day^{-1}), and surface soil moisture (%) for the Northern and Southern Mediterranean (N_MED and S_MED) and Sahara (SAH) regions under the SSP5-8.5 scenario. Curves are constructed by subtracting, for each year in the period 1850–2100, the mean value for the baseline 1981–2010. Then, a 10-year running mean is applied to smooth the resulting time series. Bold curves represent the multi-ensemble mean anomaly of the 100 km (orange) and 250 km (blue) resolutions, color shadings show the envelope between the maximum and minimum values (light shading) and between the 25th and 90th percentiles (dark shading). In order to assess the significance of the discrepancies between the two different resolutions, we performed the Wilcoxon–Mann–Whitney test to compare 100- and 250-km ensemble time series by dividing the future period into four sub-periods. The horizontal dotted red curves indicate the sub-periods where the test is significant at a 95% threshold.

moistening trend over the South-Eastern Sahara for the next decades. To what extent precipitation and evapotranspiration changes may be explained by circulation changes and/or by the direct response of the hydrological cycle to the increase in global temperature and how this will vary in time and space remain open questions. Tuel et al., (2021) show that CMIP5 GCMs project the development of a strong winter anticyclone centered on the Mediterranean Sea that results from a combination of large-scale shifts in winter planetary waves and to the reduced warming of the sea with respect to the surrounding lands. This anticyclonic anomaly and the associated dry advection effect over North Africa and S_MED may explain most of the decrease in precipitation in this

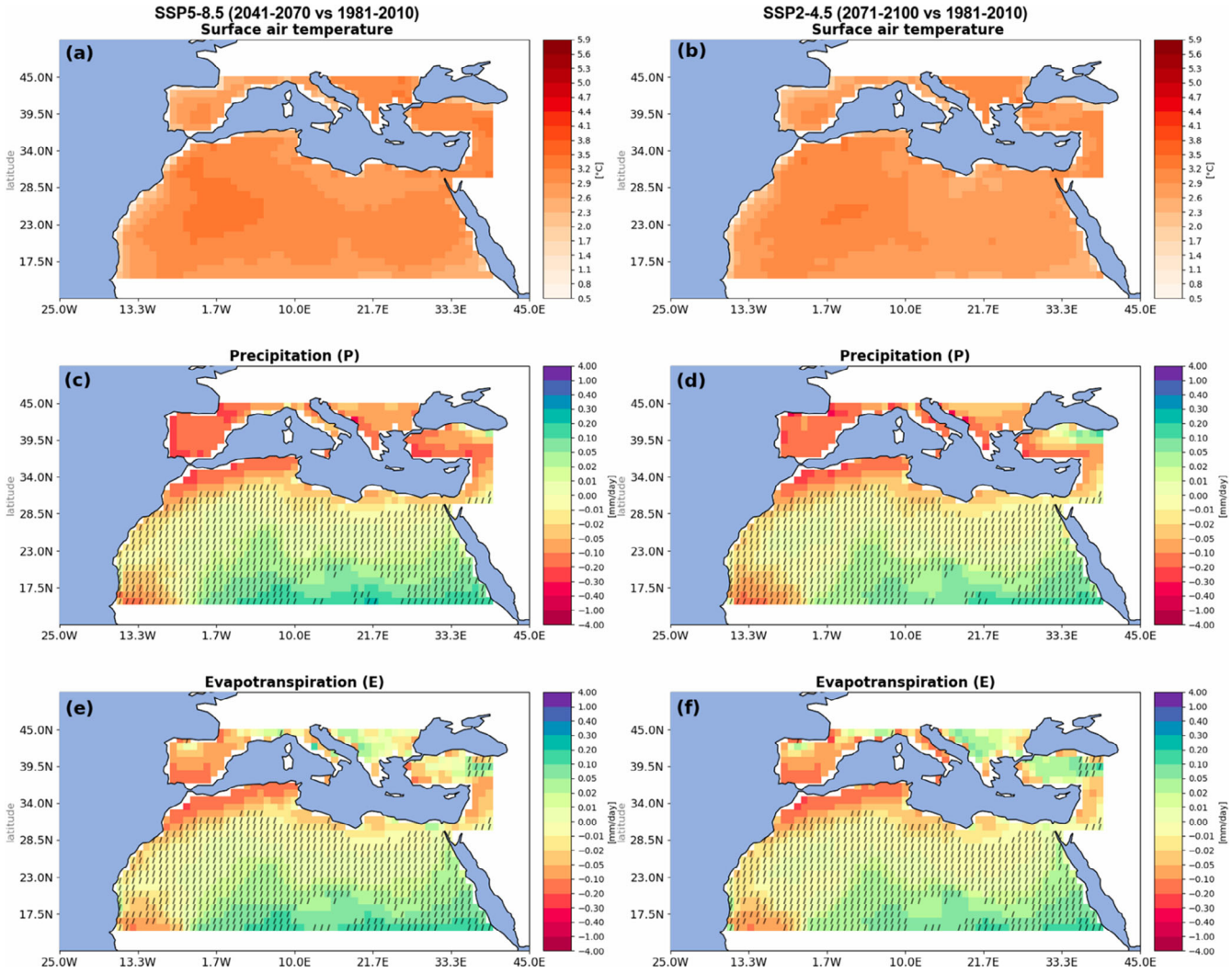

FIGURE 5 Mean future changes from the 100-km ensemble of annual surface air temperature (°C), precipitation (mm day^{-1}) and evapotranspiration (mm day^{-1}). Panels in the left column show the differences between the 2041–2070 and 1981–2010 periods for the SSP5-8.5 while those in the right column show the differences between the 2071–2100 and 1981–2010 periods for the SSP2-4.5. Hatches indicate grid boxes where the high-end and low-end changes are not statistically different based on the nonparametric Wilcoxon–Mann–Whitney with a 95% threshold.

region. Drobinski et al., (2020) also underlined that the aridification over the Sahara and IP cannot be solely explained by the increase in temperature and that the development of local circulations associated with the faster increase in temperature over land plays a significant role.

To explore the behavior of the CMIP6 simulations concerning this aspect, we compare the evolution of the surface water budget under a fastly-warming and a slowly-warming scenario for a given increment in mean global temperature. The increase in mean global temperature between the 2041–2070 period and the 1981–2010 period under the SSP5-8.5 in the CMIP6 model ensemble (∼2.89 K) is very close to the increase in mean global land temperature between the 2075–2100 and 1981–2010 under the SSP2-4.5 scenario (∼ 2.90 K). The future change by the mid-century (2041–2070 vs. 1981–2010) for the high-end scenario (left panels in Figure 5), compared to the end of the century (2071–2100 vs. 1981–2100) for the SSP2-4.5 scenario (right panels in Figure 5) is, therefore, assessed for P, E and the mean surface air temperature for the 100-km resolution ensemble. The overall near-surface temperature change over MED and SAH is very close between the two ensembles. Over SAH, both ensembles project a moistening, P and E do not significantly change and the two ensembles do not show statistically different results except in some parts in the southeast. This suggests that changes in E and P over SAH are slightly or not scenario-dependent and rather respond to the overall temperature increase. Regarding

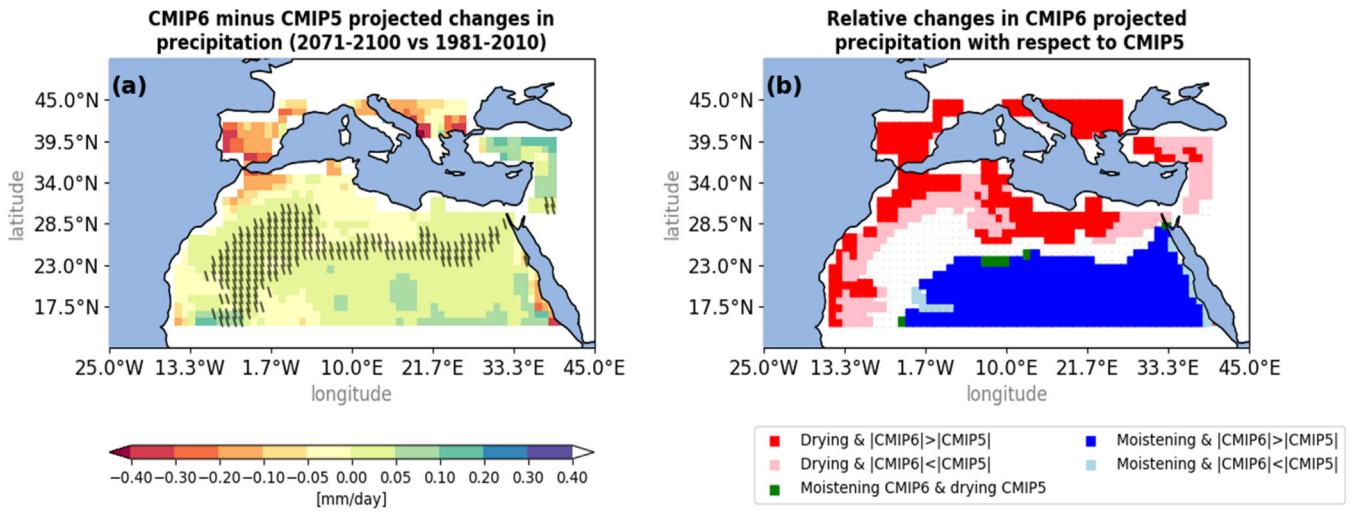

FIGURE 6 Panel (a): CMIP6 minus CMIP5 model ensemble projection of mean annual precipitation change between 2071–2100 and 1981–2010. Backslashes indicate the grid boxes corresponding to statistically insignificant differences based on the non-parametric Wilcoxon–Mann–Whitney with a 95% threshold. The color shading in panel (b) qualitatively shows how the changes of precipitation projected by CMIP6 models compare with those from CMIP5 models. Dark red (respectively, dark blue) regions are where CMIP5 models predict a decrease or drying (respectively, increase or moistening) and for which CMIP6 models predict an even stronger decrease (respectively, increase) by the end of the century. Light red (respectively, light blue) regions are where the CMIP5 models ensemble projects a decrease or drying (respectively, increase or moistening) and where the CMIP6 models ensemble projects a less intense decrease (respectively, increase). Green pixels are regions where CMIP5 models project a decrease or drying and where CMIP6 models project an increase.

the Mediterranean basin, results show statistically different projections of P and E even if the geographical patterns are qualitatively alike. Changes in P and E are therefore scenario dependent and cannot be directly related to the net increment of global near-surface temperature. In line with Drobinski et al. (2020) and Tuel et al. (2021), CMIP6 models thus suggest local land heating differences—such as over Morocco (see Figure 5a, b)—and changes in circulation likely superimpose on the overall temperature increase signal to explain the future Mediterranean drying. Further investigation into those physical and dynamical mechanisms is needed, considering for instance seasonal aspects (Brogli et al., 2019) but it is beyond the scope of the present paper.

3.5 | Projected changes in CMIP6 compared to CMIP5

Prior to concluding this letter, it is worth examining to what extent our CMIP6-based results differ or concur with CMIP5 projections. We thus compare CMIP6 and CMIP5 results under high-end forcing over the MED and SAH regions, with a particular focus on precipitation. Figure 6a shows CMIP6 and CMIP5 differences in future projected precipitation (CMIP6 minus CMIP5). Results show more intense changes than in CMIP5. This former shows less intense future precipitation increase over SAH with differences ranging to $+0.3$ mm day^{-1}. This concurs with Almazroui et al., (2020) who found intense mean annual precipitation in CMIP6 compared to CMIP5 over Sahara. Differences in precipitation extends up to -0.2 mm day^{-1} across the Northern parts of Morocco and Algeria, Mauritanian coasts, and N_MED. Indeed, Figure 6b shows that CMIP6 and CMIP5 precipitation changes generally agree on the sign of the change. However, the projected drying is more intense in CMIP6 over western N_MED, Northern Morocco and Libya, and Atlantic coasts of Mauritanians, the Saharan moistening is also more intense in CMIP6. Similar results have also been found in previous studies (e.g., Chen et al., 2020; Lee et al., 2021). CMIP6 models project intense globally-averaged surface air temperature (GSAT) increase in comparison with CMIP5 (Lee et al., 2021)—in particular, due to a higher climate sensitivity of models (Meehl et al. 2020)—the change in several climate quantities such as large-scale precipitation scales with GSAT signal (Lee et al., 2021).

4 | SUMMARY AND CONCLUSIONS

CMIP6 models project a robust decrease in precipitation over MED by the end of the century with larger uncertainty across Southern Morocco and Mauritania. An

opposite behavior is projected in South-Eastern Sahara with a relative increase in precipitation in all models. Evapotranspiration behavior follows the precipitation pattern with weaker intensity over N_MED, resulting in a negative projected freshwater flux over this region and a near-zero projected P-E over S_MED and Sahara. The future negative freshwater flux over MED may exacerbate existing water scarcity issues, particularly in areas heavily reliant on agriculture (García-Ruiz et al., 2011). These changes may also have implications in terms of wildfire which is already a significant risk in the Mediterranean region (Rovithakis et al., 2022; Turco et al., 2018). Interestingly, the projected increase in precipitation over South-Eastern Sahara does not result in a climatological increase in P–E which means that the net surface water availability is not projected to increase. This may have important implications for the future of water resources in this region but this result should be interpreted with caution. In fact, the increase in evapotranspiration that balances precipitation does not necessarily translate into a net loss of water, it may have the potential to support increased plant transpiration leading to a boost in vegetation growth in the region. The seasonal analysis also reveals a contrasted evolution with a relative increase in P–E in summer and a decrease in winter, the main rainy season, over North Africa. Such an evolution has potential implications regarding the adaptation to the future of the water resources in the region, for instance, rainwater harvesting, water storage facilities, and efficient water management and irrigation systems.

A preliminary analysis has revealed that the 100-km resolution models project less intense drying over MED with a less intermodel spread in comparison with the 250-km resolution models. However, those results should be interpreted with caution since the differences between the two ensembles are not only explained by the difference in resolution. Further work focusing on scenarios performed with one given model at various resolutions would help assess in a more robust way the effective sensitivity to resolution.

A brief complementary analysis suggests a higher scenario-dependency of the hydrological cycle changes over the Mediterranean than over the Sahara where changes seem more directly related to the overall global increase in temperature. Moreover, while the CMIP6 model ensemble qualitatively agrees with the CMIP5 ensemble in terms of precipitation projection, the magnitude of the projected changes is generally higher in CMIP6, with a more intense drying over MED and more intense moistening over the Sahara.

Our results allow us to identify robust signals in future model projections over the Mediterranean and North Africa even though on a regional scale, climate change depends on the ability of models to properly simulate the main atmospheric circulation patterns. Further studies making use of empirical bias-corrections methods (Krinner et al., 2020) would make it possible to further strengthen the reliability of GCM-based regional projections over the MED and SAH regions. Future scenarios over North Africa would also benefit from fostering the development and evaluation of model parameterizations and configurations specifically adapted for Africa, as models are generally insufficiently developed and evaluated for this continent (James et al., 2018).

AUTHOR CONTRIBUTIONS

Khadija ARJDAL: Investigation; software; visualization; writing – original draft; writing – review and editing. **Fatima Driouech:** Conceptualization; methodology; project administration; supervision; writing – original draft; writing – review and editing. **Étienne Vignon:** Methodology; supervision; writing – original draft; writing – review and editing. **Frédérique Cheruy:** Conceptualization; writing – review and editing. **Rodrigo Manzanas:** Methodology; writing – original draft; writing – review and editing. **Philippe Drobibski:** Methodology; writing – review and editing. **Abdelghani Chehbouni:** Project administration; writing – review and editing. **Abderrahmane Idelkadi:** Software; writing – review and editing.

ACKNOWLEDGEMENTS

We gratefully thank Frédéric Hourdin and Laurent Li for insightful discussions as well as Cécile Agosta for providing evaluation scripts to assess the reliability of large-scale circulation fields in CMIP6 simulations. This study was conducted using the ESPRI (Ensemble de Services Pour la Recherche l'IPSL) computing and data center (https://mesocentre.ipsl.fr) which is supported by CNRS, Sorbonne Université, École Polytechnique, and CNES and through national and international grants. We also thank the UM6P-X project for financing this work.

FUNDING INFORMATION

This work was conducted in the context of Khadija Arjdal's doctoral program funded by Mohammed VI Polytechnic University (UM6P) in the framework of the UM6P and l'Institut Polytechnique de Paris (l'X) collaboration project on climate modeling.

CONFLICT OF INTEREST STATEMENT

The authors declare that they have no competing interests.

DATA AVAILABILITY STATEMENT

The CMIP6 and CMIP5 data are accessible via the Earth System Grid Federation (https://esgf-node.llnl.gov/search/cmip6/ and https://esgf-node.llnl.gov/search/cmip5/).

ORCID

Khadija Arjdal https://orcid.org/0000-0002-2790-3790
Fatima Driouech https://orcid.org/0000-0002-0830-1831
Étienne Vignon https://orcid.org/0000-0003-3801-9367
Frédérique Chéruy https://orcid.org/0000-0003-2833-7273
Rodrigo Manzanas https://orcid.org/0000-0002-0001-3448
Philippe Drobinski https://orcid.org/0000-0002-8667-9899
Abdelghani Chehbouni https://orcid.org/0000-0002-0270-1690

REFERENCES

Agosta, C., Fettweis, X. & Datta, R. (2015) Evaluation of the CMIP5 models in the aim of regional modelling of the Antarctic surface mass balance. *The Cryosphere*, 9, 2311–2321. Available from: https://doi.org/10.5194/tc-9-2311-2015

Almazroui, M., Saeed, F., Saeed, S., Nazrul Islam, M., Ismail, M., Klutse, N.A.B. et al. (2020) Projected change in temperature and precipitation over Africa from CMIP6. *Earth Systems and Environment*, 4(3), 455–475. Available from: https://doi.org/10.1007/s41748-020-00161-x

Ashfaq, M., Rastogi, D., Mei, R., Kao, S.-C., Gangrade, S., Naz, B.S. et al. (2016) High-resolution ensemble projections of near-term regional climate over the continental United States: Climate projections over the US. *Journal of Geophysical Research: Atmospheres*, 121(17), 9943–9963. Available from: https://doi.org/10.1002/2016JD025285

Babaousmail, H., Hou, R., Ayugi, B., Ojara, M., Ngoma, H., Karim, R. et al. (2021) Evaluation of the Performance of CMIP6 Models in Reproducing Rainfall Patterns over North Africa. *Atmosphere*, 12(4), 475. Available from: https://doi.org/10.3390/atmos12040475

Bağçaci, S.Ç., Yucel, I., Duzenli, E. & Yilmaz, M.T. (2021) Intercomparison of the expected change in the temperature and the precipitation retrieved from CMIP6 and CMIP5 climate projections: A Mediterranean hot spot case. *Turkey. Atmospheric Research*, 256, 105576. Available from: https://doi.org/10.1016/j.atmosres.2021.105576

Balhane, S., Driouech, F., Chafki, O., Manzanas, R., Chehbouni, A. & Moufouma-Okia, W. (2021) Changes in mean and extreme temperature and precipitation events from different weighted multi-model ensembles over the northern half of Morocco. *Climate Dynamics*, 58, 389–404. Available from: https://doi.org/10.1007/s00382-021-05910-w

Boucher, O., Servonnat, J., Albright, A.L., Aumont, O., Balkanski, Y., Bastrikov, V. et al. (2020) Presentation and Evaluation of the IPSL-CM6A-LR Climate Model. *Journal of Advances in Modeling Earth Systems*, 12(7), Portico. Available from: https://doi.org/10.1029/2019ms002010

Brogli, R., Sørland, S.L., Kröner, N. & Schär, C. (2019) Causes of future Mediterranean precipitation decline depend on the season. *Environmental Research Letters*, 14(11), 114017. Available from: https://doi.org/10.1088/1748-9326/ab4438

Byrne, M.P. & O'Gorman, P.A. (2015) The Response of Precipitation Minus Evapotranspiration to Climate Warming: Why the "Wet-Get-Wetter, Dry-Get-Drier" Scaling Does Not Hold over Land*. *Journal of Climate*, 28(20), 8078–8092. Available from: https://doi.org/10.1175/jcli-d-15-0369.1

Chen, H., Sun, J., Lin, W. & Xu, H. (2020) Comparison of CMIP6 and CMIP5 models in simulating climate extremes. *Science Bulletin*, 65(17), 1415–1418. Available from: https://doi.org/10.1016/j.scib.2020.05.015

Cherchi, A., Fogli, P.G., Lovato, T., Peano, D., Iovino, D., Gualdi, S. et al. (2018) Global mean climate and main patterns of variability in the CMCC-CM2 coupled model. *Journal of Advances in Modeling Earth Systems*, Portico. Available from: https://doi.org/10.1029/2018ms001369

Cherif, S., Doblas-Miranda, E., Lionello, P., Borrego, C., Giorgi, F., Iglesias, A. et al. (2020) Drivers of Change (Climate and Environmental Change in the Mediterranean Basin—Current Situation and Risks for the Future First Mediterranean Assessment Report (MAR1)) (p. 128).

Cook, B.I., Mankin, J.S., Marvel, K., Williams, A.P., Smerdon, J.E. & Anchukaitis, K.J. (2020) Twenty-first century drought projections in the CMIP6 forcing scenarios. *Earth's Future*, 8(6), 1–20. Available from: https://doi.org/10.1029/2019EF001461

Diffenbaugh, N.S. & Giorgi, F. (2012) Climate change hotspots in the CMIP5 global climate model ensemble. *Climatic Change*, 114, 813–822. Available from: https://doi.org/10.1007/s10584-012-0570-x

Douville, H. & John, A. (2021) Fast adjustment versus slow SST-mediated response of daily precipitation statistics to abrupt 4xCO2. *Climate Dynamics*, 56(3–4), 1083–1104. Available from: https://doi.org/10.1007/s00382-020-05522-w

Driouech, F. (2010) Distribution des précipitations hivernales sur le Maroc dans le cadre d'un changement climatique: descente d'échelle et incertitudes.

Driouech, F., Mahé, G., Déqué, M., Dieulin, C., Heirech, T.E., Milano, M. et al. (2010) Evaluation d'impacts Potentiels de Changements Climatiques Sur l'hydrologie du Bassin Versant de la Moulouya au Maroc, 8.

Drobinski, P., da Silva, N., Bastin, S., Mailler, S., Muller, C., Ahrens, B. et al. (2020) How warmer and drier will the Mediterranean region be at the end of the twenty-first century? *Regional Environmental Change*, 20(3), 78. Available from: https://doi.org/10.1007/s10113-020-01659-w

Eyring, V., Bony, S., Meehl, G.A., Senior, C.A., Stevens, B., Stouffer, R.J. et al. (2016) Overview of the coupled model Intercomparison project phase 6 (CMIP6) experimental design and organization. *Geoscientific Model Development*, 9(5), 1937–1958. Available from: https://doi.org/10.5194/gmd-9-1937-2016

García-Ruiz, J.M., López-Moreno, J.I., Vicente-Serrano, S.M., Lasanta-Martínez, T. & Beguería, S. (2011) Mediterranean water resources in a global change scenario. *Earth-Science Reviews*, 105, 121–139. Available from: https://doi.org/10.1016/j.earscirev.2011.01.006

Gutjahr, O., Putrasahan, D., Lohmann, K., Jungclaus, J.H., von Storch, J.-S., Brüggemann, N. et al. (2019) Max Planck Institute Earth System Model (MPI-ESM 1.2) for the High-Resolution Model Intercomparison Project (High Res MIP). *Geoscientific Model Development*, 12(7), 3241–3281. Available from: https://doi.org/10.5194/gmd-12-3241-2019

Hanel, M., Rakovec, O., Markonis, Y., Máca, P., Samaniego, L., Kyselý, J. et al. (2018) Revisiting the recent European droughts from a long-term perspective. *Scientific Reports*, 8(1), 9499. Available from: https://doi.org/10.1038/s41598-018-27464-4

IPCC. (2021) In: Masson-Delmotte, V., Zhai, P., Pirani, A., Connors, S.L., Péan, C., Berger, S. et al. (Eds.) *Summary for Policymakers. In: Climate Change 2021: The Physical Science Basis. Contribution of Working Group I to the Sixth Assessment Report of the Intergovernmental Panel on Climate Change*. Cambridge: Cambridge University Press. In Press.

Iturbide, M., Gutiérrez, J.M., Alves, L.M., Bedia, J., Cimadevilla, E., Cofiño, A.S. et al. (2020) An update of IPCC climate reference regions for subcontinental analysis of climate model data: definition and aggregated datasets (preprint). Data, Algorithms, and Models. https://doi.org/10.5194/essd-2019-258

James, R., Washington, R., Abiodun, B., Kay, G., Mutemi, J., Pokam, W. et al. (2018) Evaluating climate models with an African lens. *Bulletin of the American Meteorological Society*, 99(2), 313–336. Available from: https://doi.org/10.1175/BAMS-D-16-0090.1

Kelley, M., Schmidt, G.A., Nazarenko, L.S., Bauer, S.E., Ruedy, R., Russell, G.L. et al. (2020) GISS-E2.1: Configurations and Climatology. *Journal of Advances in Modeling Earth Systems*, 12(8), Portico. Available from: https://doi.org/10.1029/2019ms002025

Krinner, G., Kharin, V., Roehrig, R., Scinocca, J. & Codron, F. (2020) Historically-based run-time bias corrections substantially improve model projections of 100 years of future climate change. *Communications Earth & Environment*, 1(1), 29. Available from: https://doi.org/10.1038/s43247-020-00035-0

Lauritzen, P.H., Nair, R.D., Herrington, A.R., Callaghan, P., Goldhaber, S., Dennis, J.M. et al. (2018) NCAR Release of CAM-SE in CESM2.0: A Reformulation of the Spectral Element Dynamical Core in Dry-Mass Vertical Coordinates With Comprehensive Treatment of Condensates and Energy. *Journal of Advances in Modeling Earth Systems*, 10(7), 1537–1570. Portico. Available from: https://doi.org/10.1029/2017ms001257

Lee, J.-Y., Marotzke, J., Bala, G., Cao, L., Corti, S., Dunne, J.P. et al. (2021) In: Masson-Delmotte, V., Zhai, P., Pirani, A., Connors, S.-L., Péan, C., Berger, S. et al. (Eds.) *Future Global Climate: Scenario-Based Projections and NearTerm Information. In Climate Change 2021: The Physical Science Basis. Contribution of Working Group I to the Sixth Assessment Report of the Intergovernmental Panel on Climate Change*. Cambridge, United Kingdom and New York, NY, USA: Cambridge University Press, pp. 553–672. Available from: https://doi.org/10.1017/9781009157896.006

Lee, W.-L., Wang, Y.-C., Shiu, C.-J., Tsai, I., Tu, C.-Y., Lan, Y.-Y. et al. (2020) Taiwan earth system model version 1: description and evaluation of mean state. *Geoscientific Model Development*, 13(9), 3887–3904. Available from: https://doi.org/10.5194/gmd-13-3887-2020

Li, L. (2019) CAS FGOALS-g3 model output prepared for CMIP6 Scenario MIP ssp 370 (Version 20230213) [Data set]. *Earth System Grid Federation*. Available from: https://doi.org/10.22033/ESGF/CMIP6.3480

Lionello, P. & Scarascia, L. (2018) The relation between climate change in the Mediterranean region and global warming. *Regional Environmental Change*, 18(5), 1481–1493. Available from: https://doi.org/10.1007/s10113-018-1290-1

Mamalakis, A., Randerson, J.T., Yu, J.-Y., Pritchard, M.S., Magnusdottir, G., Smyth, P. et al. (2021) Zonally opposing shifts of the intertropical convergence zone in response to climate change, 45.

Marchane, A., Tramblay, Y., Hanich, L., Ruelland, D. & Jarlan, L. (2017) Climate change impacts on surface water resources in the Rheraya catchment (high atlas, Morocco). *Hydrological Sciences Journal*, 62(6), 979–995. Available from: https://doi.org/10.1080/02626667.2017.1283042

Mariotti, A., Pan, Y., Zeng, N. & Alessandri, A. (2015) Long-term climate change in the Mediterranean region in the midst of decadal variability. *Climate Dynamics*, 44(5–6), 1437–1456. Available from: https://doi.org/10.1007/s00382-015-2487-3

Mauritsen, T., Bader, J., Becker, T., Behrens, J., Bittner, M., Brokopf, R. et al. (2019) Developments in the MPI-M Earth System Model version 1.2 (MPI-ESM 1.2) and Its Response to Increasing CO 2. *Journal of Advances in Modeling Earth Systems*, 11(4), 998–1038. Portico. Available from: https://doi.org/10.1029/2018ms001400

McSweeney, C.F., Jones, R.G., Lee, R.W. & Rowell, D.P. (2015) Selecting CMIP5 GCMs for downscaling over multiple regions. *Climate Dynamics*, 44(11–12), 3237–3260. Available from: https://doi.org/10.1007/s00382-014-2418-8

Meehl, G.A., Senior, C.A., Eyring, V., Flato, G., Lamarque, J.-F., Stouffer, R.J. et al. (2020) Context for interpreting equilibrium climate sensitivity and transient climate response from the CMIP6 Earth system models. Science. *Advances*, 6(26). Available from: https://doi.org/10.1126/sciadv.aba1981

O'Neill, B.C., Tebaldi, C., van Vuuren, D.P., Eyring, V., Friedlingstein, P., Hurtt, G. et al. (2016) The scenario model Intercomparison project (ScenarioMIP) for CMIP6. *Geoscientific Model Development*, 9(9), 3461–3482. Available from: https://doi.org/10.5194/gmd-9-3461-2016

Prudhomme, C., Giuntoli, I., Robinson, E.L., Clark, D.B., Arnell, N.W., Dankers, R. et al. (2014) Hydrological droughts in the 21st century, hotspots and uncertainties from a global multimodel ensemble experiment. *Proceedings of the National Academy of Sciences*, 111(9), 3262–3267. Available from: https://doi.org/10.1073/pnas.1222473110

Rong, X.Y., Li, J., Chen, H.M. et al. (2019) Introduction of CAMS-CSM model and its participation in CMIP6. *Clim Change Res*, 15(5), 540–544. Available from: https://doi.org/10.12006/j.issn.1673-1719.2019.186

Rovithakis, A., Grillakis, M.G., Seiradakis, K.D., Giannakopoulos, C., Karali, A., Field, R. et al. (2022) Future climate change impact on wildfire danger over the Mediterranean: the case of Greece. *Environmental Research Letters*, 17(4), 045022. Available from: https://doi.org/10.1088/1748-9326/ac5f94

Ruosteenoja, K., Markkanen, T., Venäläinen, A., Räisänen, P. & Peltola, H. (2018) Seasonal soil moisture and drought occurrence in Europe in CMIP5 projections for the 21st century. *Climate Dynamics*, 50(3–4), 1177–1192. Available from: https://doi.org/10.1007/s00382-017-3671-4

Séférian, R., Nabat, P., Michou, M., Saint-Martin, D., Voldoire, A., Colin, J. et al. (2019) Evaluation of CNRM Earth System Model, CNRM-ESM 2-1: Role of Earth System Processes in Present-Day and Future Climate. *Journal of Advances in Modeling Earth Systems*, 11(12), 4182–4227. Portico. Available from: https://doi.org/10.1029/2019ms001791

Seker, M. & Gumus, V. (2022) Projection of temperature and precipitation in the Mediterranean region through multi-model ensemble from CMIP6. *Atmospheric Research*, 280, 106440. Available from: https://doi.org/10.1016/j.atmosres.2022.106440

Seland, Ø., Bentsen, M., Seland Graff, L., Olivié, D., Toniazzo, T., Gjermundsen, A. et al. (2020) *The Norwegian Earth System Model, Nor ESM2 – Evaluation of the CMIP6 DECK and historical simulations*. https://doi.org/10.5194/gmd-2019-378

Sellar, A.A., Jones, C.G., Mulcahy, J.P., Tang, Y., Yool, A., Wiltshire, A. et al. (2019) UKESM1: Description and Evaluation of the U.K. Earth System Model. *Journal of Advances in Modeling Earth Systems*, 11(12), 4513–4558. Portico. Available from: https://doi.org/10.1029/2019ms001739

Seneviratne, S.I., Corti, T., Davin, E.L., Hirschi, M., Jaeger, E.B., Lehner, I. et al. (2010) Investigating soil moisture–climate interactions in a changing climate: a review. *Earth-Science Reviews*, 99(3–4), 125–161. Available from: https://doi.org/10.1016/j.earscirev.2010.02.004

Seneviratne, S.I., Zhang, X., Adnan, M., Badi, W., Dereczynski, C., Di Luca, A. et al. (2021) In: Masson-Delmotte, V., Zhai, P., Pirani, A., Connors, S.L., Péan, C., Berger, S. et al. (Eds.) *Weather and Climate Extreme Events in a Changing Climate. In: Climate Change 2021: The Physical Science Basis. Contribution of Working Group I to the Sixth Assessment Report of the Intergovernmental Panel on Climate Change*. Cambridge: Cambridge University Press. In Press.

Tatebe, H., Ogura, T., Nitta, T., Komuro, Y., Ogochi, K., Takemura, T. et al. (2019) Description and basic evaluation of simulated mean state, internal variability, and climate sensitivity in MIROC6. *Geoscientific Model Development*, 12(7), 2727–2765. Available from: https://doi.org/10.5194/gmd-12-2727-2019

Tebaldi, C., Smith, R.L., Nychka, D. & Mearns, L.O. (2005) Quantifying uncertainty in projections of regional climate change: a Bayesian approach to the analysis of multimodel ensembles. *Journal of Climate*, 18(10), 1524–1540. Available from: https://doi.org/10.1175/JCLI3363.1

Tramblay, Y., Jarlan, L., Hanich, L. & Somot, S. (2018) Future scenarios of surface water resources availability in north African dams. *Water Resources Management*, 32(4), 1291–1306. Available from: https://doi.org/10.1007/s11269-017-1870-8

Tuel, A. & Eltahir, E.A.B. (2020) Why is the Mediterranean a climate change hot spot? *Journal of Climate*, 33(15), 5843.

Tuel, A., Kang, S. & Eltahir, E.A.B. (2021) Understanding climate change over the southwestern Mediterranean using high-resolution simulations. *Climate Dynamics*, 56(3–4), 985–1001. Available from: https://doi.org/10.1007/s00382-020-05516-8

Turco, M., Rosa-Cánovas, J.J., Bedia, J., Jerez, S., Montávez, J.P., Llasat, M.C. et al. (2018) Exacerbated fires in Mediterranean Europe due to anthropogenic warming projected with non-stationary climate-fire models. *Nature Communications*, 9(1), 3821. Available from: https://doi.org/10.1038/s41467-018-06358-z

Voldoire, A., Saint-Martin, D., Sénési, S., Decharme, B., Alias, A., Chevallier, M. et al. (2019) Evaluation of CMIP6 DECK Experiments With CNRM-CM6-1. *Journal of Advances in Modeling Earth Systems*, 11(7), 2177–2213. Portico. Available from: https://doi.org/10.1029/2019ms001683

Waha, K., Krummenauer, L., Adams, S., Aich, V., Baarsch, F., Coumou, D. et al. (2017) Climate change impacts in the Middle East and northern Africa (MENA) region and their implications for vulnerable population groups. *Regional Environmental Change*, 17(6), 1623–1638. Available from: https://doi.org/10.1007/s10113-017-1144-2

Wu, T., Lu, Y., Fang, Y., Xin, X., Li, L. & Li, W. (2019) The Beijing Climate Center Climate System Model (BCC-CSM): the main progress from CMIP5 to CMIP6. *Geoscientific Model Development*, 12(4), 1573–1600. Available from: https://doi.org/10.5194/gmd-12-1573-2019

Xoplaki, E. (2002) Climate variability over the Mediterranean (PhD thesis). Universität Bern, Switzerland.

Yukimoto, S., Kawai, H., Koshiro, T., Oshima, N., Yoshida, K., Urakawa, S. et al. (2019) The Meteorological Research Institute Earth System Model Version 2.0, MRI-ESM 2.0: Description and Basic Evaluation of the Physical Component. *Journal of the Meteorological Society of Japan*, Ser II, 97(5), 931–965. Available from: https://doi.org/10.2151/jmsj.2019-051

SUPPORTING INFORMATION

Additional supporting information can be found online in the Supporting Information section at the end of this article.

How to cite this article: Arjdal, K., Driouech, F., Vignon, É., Chéruy, F., Manzanas, R., Drobinski, P., Chehbouni, A., & Idelkadi, A. (2023). Future of land surface water availability over the Mediterranean basin and North Africa: Analysis and synthesis from the CMIP6 exercise. *Atmospheric Science Letters*, e1180. https://doi.org/10.1002/asl.1180